Journal of Biomedical Optics 5(3), 307–314 (July 2000)

On the use of schematic eye models to estimate retinal image quality

G. Li
H. Zwick
B. Stuck
D. J. Lund
Walter Reed Army Institute of Research
U.S. Army Medical Research Detachment
Brooks Air Force Base, Texas 78235-5138

Abstract. The optical performance of the eyes of nine vertebrate species was evaluated using optical system design techniques and schematic eye models. Essential features of eyes, including the modulation transfer function (MTF) and the MTF cutoff frequency are related to the numerical aperture of the eyes. Superior resolution for *in vivo* imaging of photoreceptors may be achieved by dilating the iris pupil of an eye, minimizing coherence, and using short wavelength illumination. The difference of lateral and axial resolution between a small and a large eye for imaging photoreceptors *in vivo*. [S1083-3668(00)01003-0]

Keywords: vertebrate eye; retinal image; schematic eye; resolution.

Paper JBO-90037 received July 12, 1999; revised manuscript received Nov. 29, 1999 and Apr. 3, 2000; accepted for publication Apr. 3, 2000.

1 Introduction

Recent investigations have demonstrated the ability, using a confocal scanning laser ophthalmoscope (SLO), to image photoreceptors and their modal structures in several species of snakes.[1–5] This ability is based primarily on the fact that the eyes of these species are short focal length optical systems of high optical quality. The same SLO cannot image photoreceptors in the human or rhesus monkey eye at the same resolution level as shown in Figures 1(a)–1(d) although others have imaged human photoreceptors with a high resolution fundus camera incorporating adaptive optics to correct optical aberrations of the eye.[6,7] Diagnosis and study of retinal diseases and light-induced damage processes in the retina would be much enhanced if photoreceptors in the human eye could be easily and reproducibly imaged. There is strong interest in extending the capabilities, which image photoreceptors in the snake to the point where human photoreceptors could also be imaged. Ultimately, diffraction of light, as described by physical optics, limits the ability to image photoreceptors in the eye. It is very difficult to describe an optical wave propagating through the eye's optical system using the rigorous wave theory as is necessary to accurately determine diffraction in the eye. Light diffraction in an eye has been extensively studied.[8–22] These studies were based on experimental measurements of the point spread function (PSF) and the modulation transfer function (MTF) of eyes using double pass methods.[9–12,14,15,18–20] Also, the application of the MTF for evaluating the visual quality of the human eye has been intensively studied.[9–20] These studies did not address the relationship between light diffraction in an eye and the geometrical features of the eye, for example, the curvature of the cornea.

The eye is a living optical system. The surface profiles, thickness, and index of refraction of its ocular components determine its imaging properties and its optical resolution. Early attempts to build a schematic eye were reported in 1801 and 1841.[23,24] Since then geometrical optic models and schematic eyes have been developed for describing the paraxial optical characteristics of the eye for many species.[25–33] These studies have focused on the evaluation of visual acuity and the refractive states of eyes.[25–35] The study of light diffraction in the eye using a schematic eye model to evaluate the resolving power of eyes for imaging of retinal layers and photoreceptors has not been reported. The effects of diffraction can be approximately evaluated by finding the numerical aperture (NA), the PSF, the MTF, and the MTF cutoff frequency using schematic eye models. In this paper we employed schematic eye models for several species and optical design computer software to evaluate relationships between geometrical characteristics and the effects of light diffraction. This study builds on available concepts in physiologic and physical optics which have hitherto not been associated to provide an explanation of imaging resolution of the snake eye, and to suggest ways to improve the ability to image photoreceptors in the primate and human eye.[4]

2 Methods

The selection of accurate schematic eye models was important for this study. The performance of a schematic eye model depended on the accuracy of measurement of the indices of refraction, curvature and thickness of ocular components. Nine schematic eyes were chosen; the human, the macaque (*Macaca fascicularis*), the marmoset (*Callithrix jacchus*), the rabbit, the tree shrew (*Tupaia belangeri*), the frog (*Rana esculenta*), the rat (*D. A. Strain*), the mouse (C57B1/6J) and the checkered garter snake eye (*Thamnophis m marcianus*). Except for the snake, the schematic eyes were selected from the literature.[5,23–33] A schematic eye model for the checkered garter snake was constructed based on *in vivo* and *in vitro* measurements of the curvatures of the spectacle, cornea and crystalline lens, thickness of the spectacle, cornea, crystalline lens, aqueous chamber, and axial length using a keratometer, ultrasound, slit lamp, bio-optical microscope, frozen section and paraffin section.[4] Typical pupil sizes of the monkey, rabbit,

Address all correspondence to Guo Li. Tel: 210-536-1614; Fax: 210-536-3450; E-mail: liguo@aol.com

1083-3668/2000/$15.00 © 2000 SPIE

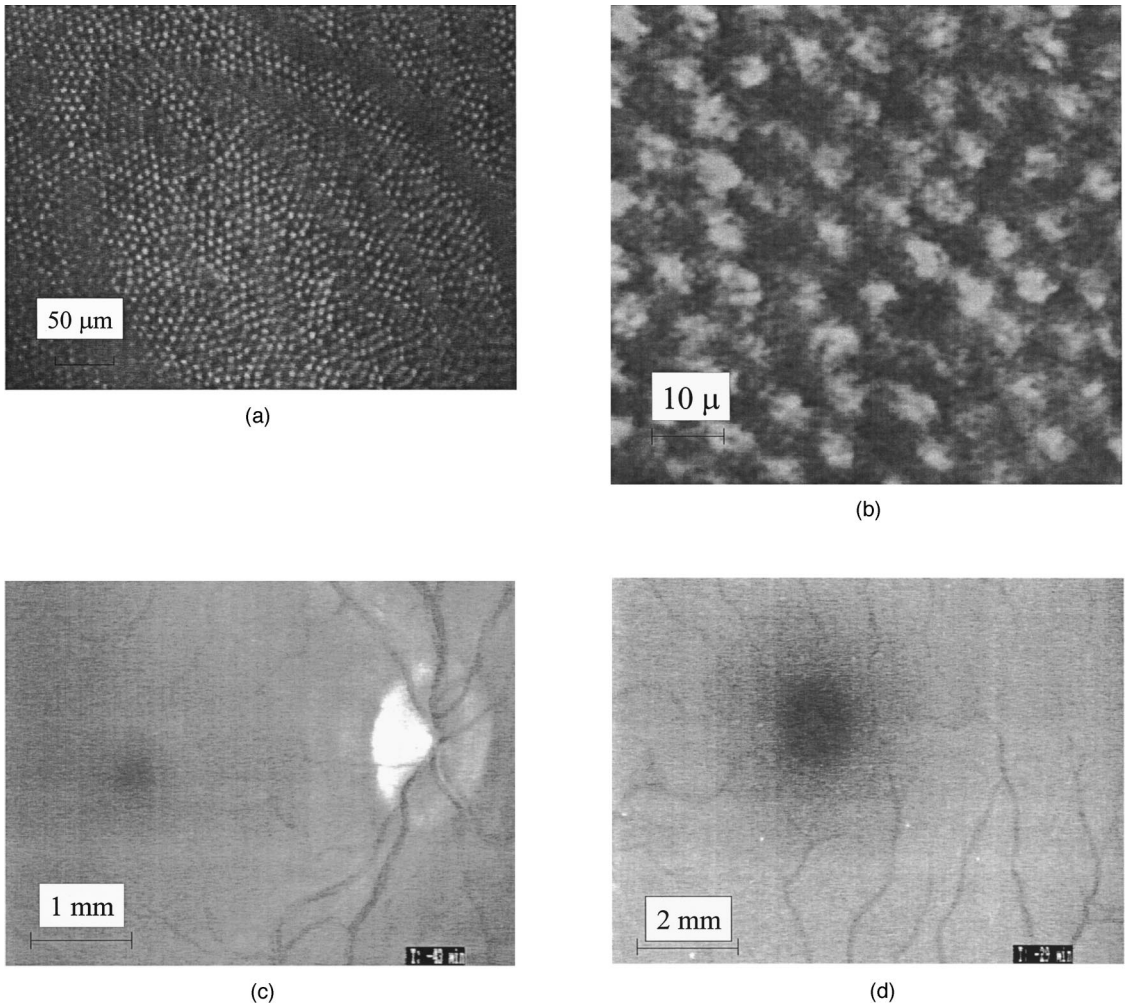

Fig. 1 (a) Photoreceptor matrix in the garter snake eye. (b) The magnified image of photoreceptors of the garter snake. (c) The human retinal image. (d) The human macular image.

frog, snake, rat and mouse eye were verified where available in the laboratory, the San Antonio zoo and local pet stores. The data about surface curvatures, and component thickness and refractive indices of these eyes were entered into the ZEMAX database for each eye. Analysis of these schematic eyes was carried out using a commercial optical design and analysis software package (ZEMAX).

When the intent was to image the retina and its components the retinal layers were in object space. The crystalline lens, pupil and cornea formed an optical system to image retinal layers or combined with ocular instruments to form images of retinal layers, for example, on the film of a Fundus camera. In this case the eye's optical system played a role like the objective lens of an optical microscope. The numerical aperture (NA) is a good indicator widely used for evaluating the resolution or resolving power of an optical microscope in industry. Also, the optical wave theory indicates that the NA is a major factor in determining the PSF of an optical system.[21,22] For a specific wavelength, the resolution is inversely proportional to the numerical aperture, or to the optical power and the effective pupil of an eye. In this study, we calculated the NA by raytracing technique, i.e., geometrical optics method then used the NA to evaluate diffraction limitation. Thus, the NA plays a key role in linking the geometric configurations and diffractive optics of small and large eyes, and in extending the concepts of geometric optics to that of diffractive optics. In the eye, the numerical aperture is defined as

$$\mathrm{NA} = n \sin U, \tag{1}$$

where n is the index of refraction of the vitreous fluid and U is the half angle of the cone defined by the pupil diameter and the effective focal length (EFL) of the eye. The effective acceptance angle, U, for each of the nine schematic eye models was obtained by ray tracing a marginal ray from an object point located at the intersection of retinal layers and the optical axis of the eye to the edge of the pupil.

The MTF is the modulus of the complex optical transfer function (OTF) and is another way to evaluate image quality, especially for continuous-tone imagery.[17,18,21,22] It is a function of optical power, numerical aperture and optical aberrations but is not simply proportional to these. The normalized MTF is a function of spatial frequencies and dropped from one at zero frequency to zero at the maximum spatial frequency. The maximum spatial frequency is also called the

cutoff spatial frequency.[21] The cutoff frequency calculated here is lateral cutoff frequency. The cutoff frequency is a function of numerical aperture and wavelength, i.e., it is equal to two times the numerical aperture divided by wavelength.[21] ZEMAX was used to compute the lateral cutoff frequency of the MTF for nine schematic eyes according to the above definitions. The MTF of the human eye was analyzed to reduce the diffraction limitation. For example, based on the analysis of the schematic eye model we anticipated that by dilating the pupil of the human eye or by using a contact lens we may improve the resolution of the living human eye available for imaging photoreceptors.

The intensity distribution of light near the focus of an error-free and rotational-symmetric optical system has been intensively studied.[21,22,36,37] The intensity distribution of light of a point image in the geometrical focal plane can be written as[21,36,37]

$$I(0,v)=I_0(2J_1(v)/v)^2, \tag{2}$$

where $J_1(v)$ is the first order of the Bessel function. The point spread function (PSF) in the meridional plane along the optical axis, z, is

$$I(u,0)=I_0[\sin(u/4)/(u/4)]^2, \tag{3}$$

where $v=2\pi/\lambda(a/f)r$ and $u=2\pi/\lambda(a/f)^2z$, I_0 is the intensity of incident light, λ wavelength, ''a'' the diameter of the pupil, f focal length and z the distance from the origin of the image space.

Stoltzman[37] discussed the PSF for different apertures and criteria. We modified his results to our case to evaluate the lateral and axial resolution or resolving power of eyes for incoherent and coherent illumination. The Rayleigh criterion is an objective criterion to evaluate the resolution for incoherent light in three-dimensional (3D) image space. Based on the Rayleigh criterion the resolution was defined such that the central peak of the normalized PSF of an ideal object point fell on the first minimum intensity of the normalized PSF of a closest object point.[21] For incoherent sources, according to the Rayleigh criterion and expression (2), the lateral resolution, R_L, i.e., the resolved separation of PSFs of two closest point images along radial direction in the focal plane, was given by[21,22,36]

$$R_L=0.6098\lambda/\mathrm{NA}, \tag{4}$$

where λ was wavelength and NA the numerical aperture.

Similarly, the closest separation of PSFs of two point images along the optical axis according to the Rayleigh criterion was determined when the intensity of a normalized PSF in expression (3) dropped from the maximum to zero. Thus, the axial resolution was expressed as

$$R_A=2.0\lambda/(\mathrm{NA})^2. \tag{5}$$

From expressions (4) and (5) we calculated the lateral and axial resolution for the nine schematic eyes using incoherent light at the wavelength $\lambda=0.587\,\mu$m.

The resolution of an optical system using a coherent source is different from that using an incoherent source because two point images formed by two coherent object points interfere with each other. The superposition of incoherent light results in the simple summation of optical intensities in the image space, whereas coherent interference results in squaring the sum of amplitudes. For a coherent source, because of the diffraction and interference effect and according to the Sparrow criterion, the lateral resolution was derived from[37]

$$(\partial^2/\partial x^2)\{(2J_1(x-u)/(x-u)+2J_1(x+u)/(x+u))^2\}|_{x=0}=0, \tag{6}$$

i.e.

$$(6-u^2)J_1(u)-3uJ_0(u)=0, \tag{7}$$

where $J_0(u)$ is the zero order of the Bessel function. We obtained $u=2.30$ by searching the roots of Eq. (7). Thus, the lateral resolution was given by

$$R_L=0.732\lambda/\mathrm{NA}, \tag{8}$$

where λ was wavelength and NA the numerical aperture. Similarly, for a coherent source the resolution along the optical axis was derived from

$$(\partial^2/\partial x^2)\{(\sin((x-u)/4)/((x-u)/4)+\sin((x+u)/4)/((x+u)/4))^2\}|_{x=0}=0. \tag{9}$$

We obtained $u=2.08$ by searching the roots of Eq. (9). Thus

$$R_A=2.65\lambda/(\mathrm{NA})^2. \tag{10}$$

From the above results, we found that the numerical aperture and the illuminating wavelength determined the lateral and axial resolution of an aberration-free optical system under both incoherent and coherent illumination.

A Rodenstock scanning laser ophthalmoscope (SLO) was employed to image photoreceptors in the checkered garter snake eye and retinal layers in the human eye. We optimized the image quality of the snake and human eye by choosing illuminating wavelength, viewing angle, and confocal aperture of the SLO, and by adjusting the video gain and refraction compensation of the SLO. External optics was employed to increase the magnification of the SLO.

3 Results

The nine chosen schematic eyes are good examples for comparison of the optical properties of large and small eyes. As an example, the schematic Human and checkered garter snake eye are shown in Figure 2. The radius of curvature of the anterior cornea of the human eye (average 7.8 mm) is about four times greater than that of the snake spectacle (1.78 mm). The axial length of the human eye is almost seven times longer than that of the checkered garter snake eye. These characteristics result in differences in effective focal length (EFL) and optical power (OP). The comparative relationship of EFL against axial length for the nine eyes is shown in Figure 3. The comparative relationship of OP against axial length for the nine eyes is shown in Figure 4.

The comparative relationship of numerical aperture on vitreous chamber length of the nine schematic eyes is shown in Figure 5. In this calculation, we consider the retinal layer as a very thin layer compared to the eye size. For a vertebrate eye the size of the pupil is relatively smaller than that of the

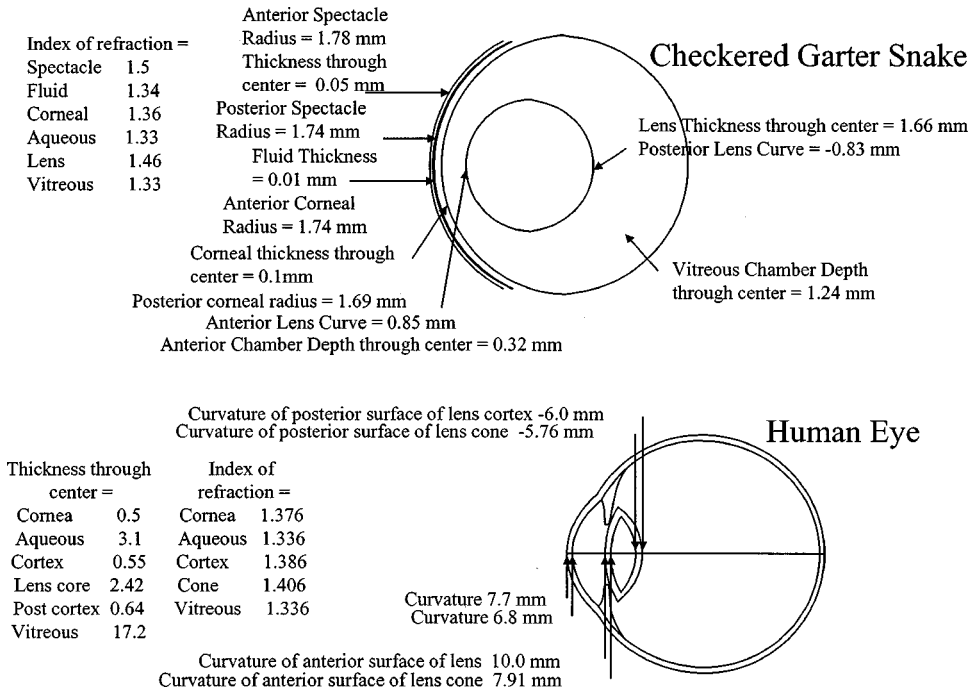

Fig. 2 The schematic eye for the human eye and checkered garter snake.

cornea and lens. For a small eye, vitreous chamber length and the radii of the corneal and lenticular surface are much smaller than those of a large eye. Thus, as shown in Figure 5, the NA of the small eye is, in general, greater than that of a large eye.

The computed MTF of the human eye as an example at 0.587 μm is shown in Figure 6. From this figure we found out the cutoff frequency of the MTF when it approached zero. The comparative relationship of lateral MTF cutoff frequency with vitreous chamber length for the nine schematic eyes is plotted in Figure 7. In these figures the unit of frequency is cycles per millimeter. This figure shows that retinal images in these eyes can in theory be resolved at micron level. A small eye has higher lateral cutoff frequency than a large eye, in general. For example, the lateral cutoff frequency of the checkered garter snake eye is about four times higher than that of the human eye.

From the MTF figure of the human eye like Figure 6, we were able to quantitatively calculate the lateral cutoff frequency of the schematic human eye as the pupil diameter changed as shown in Figure 8. The lateral cutoff frequency

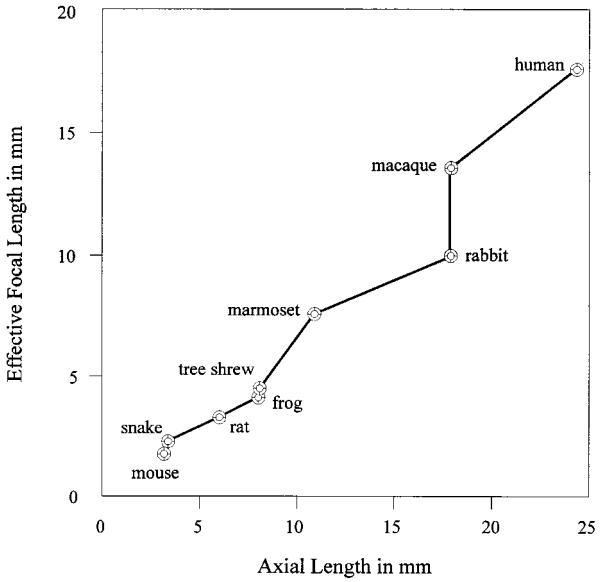

Fig. 3 The comparative relationship of effective focal length with axial length.

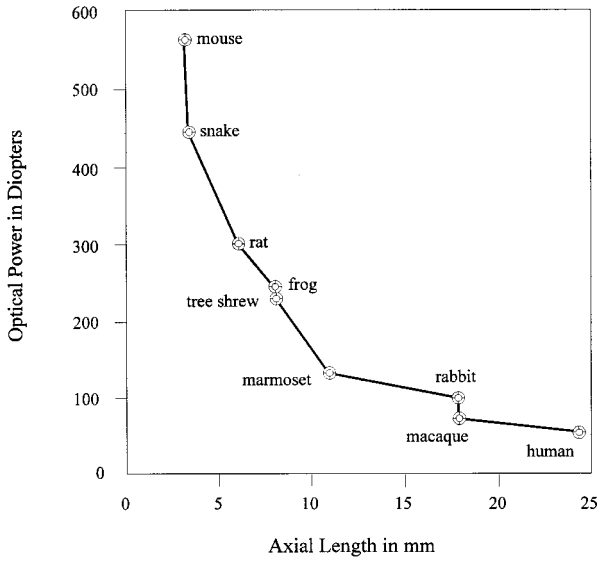

Fig. 4 The comparative relationship of optical power with axial length.

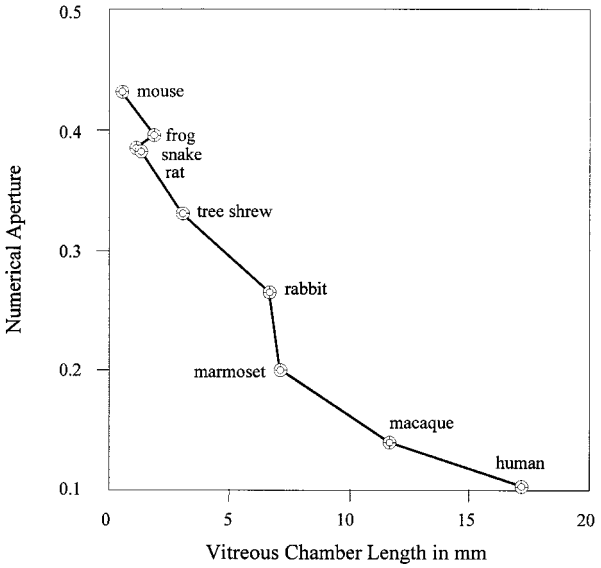

Fig. 5 The comparative relationship of numerical aperture with vitreous chamber length.

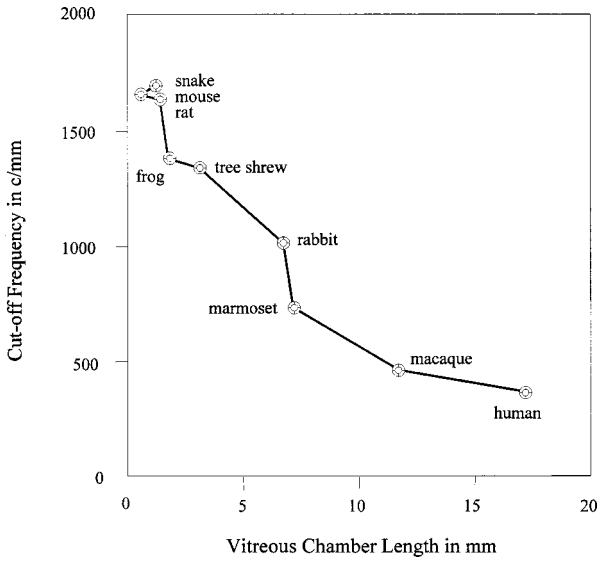

Fig. 7 The comparative relationship of cutoff frequency with vitreous chamber length.

almost linearly increases with the diameter of the pupil. For example, Figure 8 indicates that the lateral MTF cutoff frequency for the human eye is about 343 cycles per mm when the pupil size is 3.0 mm but becomes 721 cycles per mm when the pupil size increases to 6.0 mm. Thus, the resolution of the human eye may increase 2.1 times for perfect pupil dilation and good eyes.

ZEMAX was used to simulate a contact lens inserted before the anterior corneal surface of the human eye. The posterior surface of a contact lens was assumed to be in close contact with the corneal issue. For this simulation, the thickness of the contact lens was 1.15 mm, its index of refraction was 1.43 and its primary curvature was a variable. Optimizing this optical system increased the numerical aperture and cutoff frequency slightly when compared to the eye model without the contact lens. However, the optical aberrations may be very much reduced. Thus, a contact lens may be used for correcting optical aberrations of the eye for better retinal images.

The lateral and axial resolution of the nine schematic eyes, using incoherent and coherent light at the wavelength $\lambda = 0.587\,\mu$m, are plotted in Figures 9 and 10, respectively. From the two figures we see that, compared to a large eye, a small eye has better lateral and axial resolution because of higher numerical aperture. For example, the lateral resolution for the checkered garter snake eye is about 3.8 times higher than that for the human eye. Also, for the same eye under incoherent illumination the resolution is better than under coherent illumination. The lateral resolution for the same eye and light source is better than axial resolution.

The photoreceptors in the checkered garter snake eye and the Great Plains rat snake eye were imaged. SLO images of photoreceptors in the snake eye are shown in Figures 1(a) and 1(b). Figure 1(a) was imaged using a 20° field. The viewing

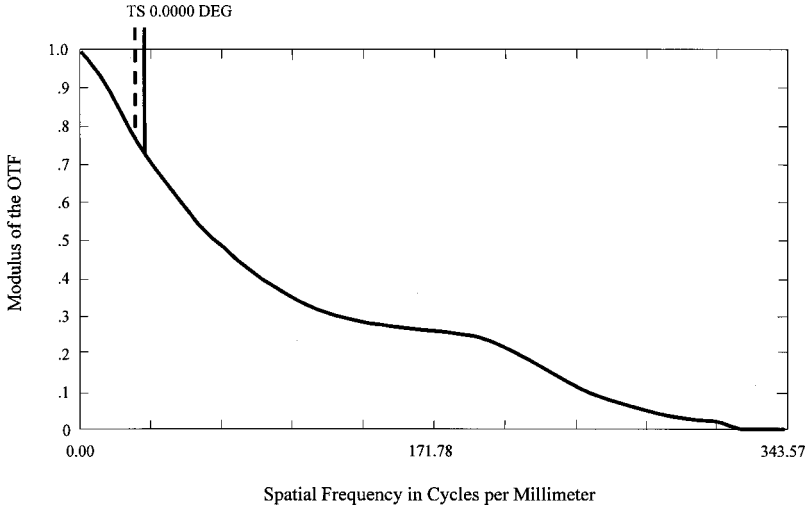

Fig. 6 The MTF of the human eye.

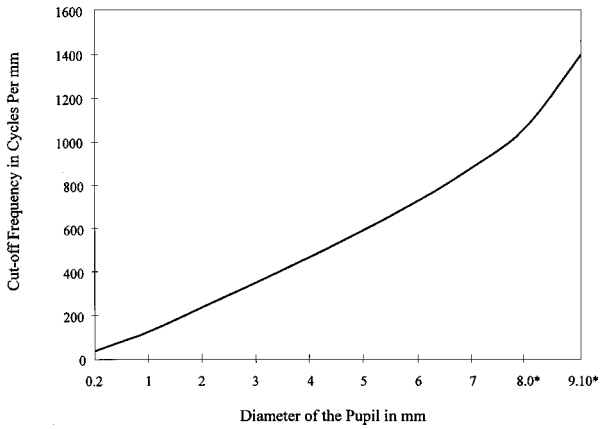

Fig. 8 The dependence of cutoff frequency on diameter of the pupil in the human eye.

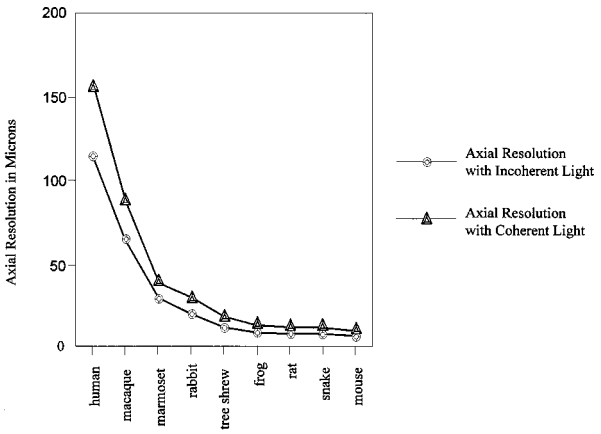

Fig. 10 Comparative axial resolution with different species.

field for Figure 1(b) was less than 10°. Large cones about 7–9 μm in size, small cones about 2–4 μm in size, double cones, and modal patterns stemming from the waveguide effect were imaged clearly as shown in the figures. An external optical system was used to magnify the images of photoreceptors of the snake eye from four to eight times greater so that a higher order of modal patterns in photoreceptors of the snake eye can be imaged clearly as shown in Figures 1(a) and 1(b). The SLO images of the human retina are shown in Figures 1(c) and 1(d). A 40° field was chosen to image the human retina as shown in Figure 1(c). A 20° field was chosen to image the human macula as shown in Figure 1(d).

4 Discussion

The above theoretical analysis and experimental results reveal the relationships of optical power, numerical aperture, MTF and lateral MTF cutoff frequencies with geometrical configurations in small and large eyes. It is easier to observe photoreceptors and modal patterns in a small eye such as the snake eye shown in Figures 1(a) and 1(b). Comparing the experimental results using the same SLO, for example, as shown in Figures 1(a)–1(d) we see that the difference of resolution in a small and large eye is great. For the nine schematic eyes we found the almost monotonic relationship of effective focal length and optical power on axial length. We also found the almost monotonic relationship of numerical aperture and lateral MTF cutoff frequency on vitreous chamber length. However, some exceptions exist. For example, the axial length of the rabbit eye is longer than that of the marmoset eye but its vitreous chamber length is shorter than that of the marmoset eye. The rabbit eye has a thicker crystalline lens and larger pupil. Thus, its optical power is higher than would be expected. Also, the numerical aperture and cutoff frequency of the rabbit eye are higher than those of the marmoset eye. It is difficult to make clear demarcation between a large and small eye only according to axial lens or vitreous chamber length because there are many animal species with very different eye configurations, structure and optical characteristics. We consider the human eye and monkey eye as ''large eye'' but the frog eye, rat eye and snake eye as ''small eye.'' The numerical aperture of a small eye is about 0.2 or greater and that of a large eye about 0.15 or less in this analysis. The optical characteristics of an eye are related to the synthesis or topology of geometrical configuration and refractive state. Hughes discussed the topography of vision in animals.[25] We developed the topography of retinal images and diffraction effect in vertebrate eyes.

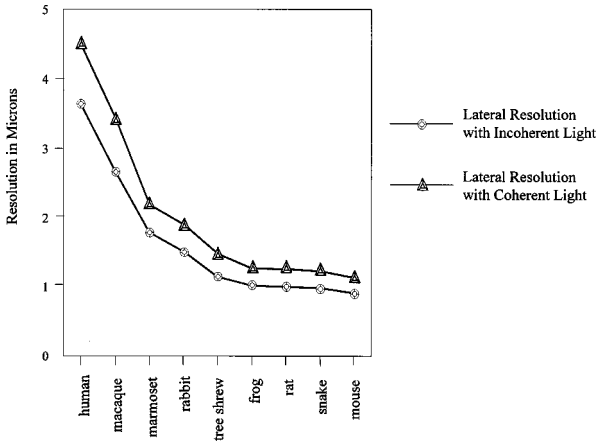

Fig. 9 Comparative lateral resolution with different species.

We calculated the lateral MTF cutoff frequency for each eye using a single-pass ray tracing technique. Thus, the MTFs calculated here are single-pass MTFs and related to the geometrical configuration of the eye. If each surface and index of refraction of the ocular components are determined very accurately, these single-pass MTFs are more objective than those evaluated by the double-pass method. The measured double-pass MTFs include double-pass optical aberrations and the interaction effects of light with retinal layers but the computed single-pass MTFs do not. When we did on-axis ray tracing and realized there were some lower order spherical aberrations in an eye. The MTF is sensitive to these aberrations but the numerical aperture is not.[21] Also, because the accuracy of ZEMAX is not very satisfactory we did not work on the MTF for all nine animals in detail.[21] For imaging photoreceptors in the central portion of the retina or some lower aberration eyes, the above studies on resolution evaluation are good approximations. Another issue related to the accuracy of this analysis is the existence of nonuniform distribution or

gradient of index of refraction in the crystalline lens. The assumed average index of refraction in the homogeneous crystalline lens has the equivalent effect of an index-gradient crystalline lens. For a good schematic model such as the human schematic eye model this approximation is adequate. However, it is difficult to measure the index of refraction of the lens in a small eye and this assumption may give rise to some errors.

Both four surface and six surface schematic eye models have been applied for this analysis. The four surface schematic eye model was applied for the macaque, marmoset, rabbit, tree shrew, frog, rat and mouse eye. In the six surface schematic eye model the lens core and lens cortex are homogeneous but with different index of refraction. The four surface and six surface schematic model for the human are in good agreement because of the relative small pupil size comparing to the lens and cornea size. We chose the six surface schematic eye model for the human eye for better accuracy. Because of the existence of the spectacle in the snake eye, the six surface schematic eye model for the checkered garter snake eye was employed.

We chose different criteria to evaluate the resolution of an eye using incoherent and coherent sources. The Rayleigh criterion is a more objective and stringent criterion than the Sparrow criterion used for incoherent light. We chose the Sparrow criterion due to the simplicity of mathematical calculation. All these criteria presume an ideal case that requires the retina to be illuminated uniformly, and the retina reflects and backscatters the illuminating light uniformly in all directions. In this condition, two closest PSFs have the same distribution or shape. Thus, the actual resolution of a real eye might be a little bit worse than our estimation.

The experimental lateral resolution for the snake eye is between 1 and 2 μm because 2 μm small cones and modal patterns have been observed by SLOs. From Eq. (9), the calculated lateral resolution using 0.587 μm coherent light for imaging photoreceptors in the checkered garter snake is about 1.21 μm. Thus, this estimation explains the experimental results very well. Comparing to the double-pass measurements which give the cutoff frequency of the human eye ranging from 60 to 150 c/deg,[6,16] our calculated cutoff frequency about 343 c/mm, (102 c/deg, 3.0 mm pupil, 0.587 μm wavelength of illumination) is a very reasonable result. According to expression (4), the calculated lateral resolution using an incoherent source for the human eye is about 3.60 μm if the illuminating wavelength is 0.587 μm. The average size of cones in the human fovea is about 2.5 μm. Thus, photoreceptors in most of the human eyes are not easily observed through a natural pupil by a conventional fundus camera. Exceptionally, photoreceptors in a few very high quality human eyes have been observed. We calculated that the lateral resolution of the human eye becomes 2.12 μm when the pupil changes from 3.0 to 6.0 mm. The possibility of imaging photoreceptors in the human eye will increase by increasing the effective pupil of an eye and using an incoherent light source of short wavelength.[1,2] Thus, photoreceptors in the human eye may be observed as the theoretical estimation and were imaged experimentally.[1,2]

We did not discuss the interaction of light with the retinal tissue, for example, backscattering, reflection, transmission, absorption and waveguide effect. These light–tissue interactions affect the ability to image photoreceptors and should not be ignored. The snake eye has a high numerical aperture and also clear media so that photoreceptors and modal patterns are imaged. However, the mouse eye, with high numerical aperture, has turbid media and small photoreceptors ranging from 0.9 to 1.1 μm. Photoreceptors in this eye have not been imaged. The different approach related to aliasing and the sampling theory also is another way to evaluate the resolution of photoreceptor mosaic. Because of the limitation of this paper we have to concentrate our discussion on the eye optics that plays the most important role for imaging photoreceptors in a small and large eye.

5 Conclusion

While *in vivo* imaging of photoreceptors in primate eyes remains difficult, the chances of success can be improved by dilating the pupil to increase the effective aperture, using a contact lens to cancel cornea induced aberrations and correct refractive errors, and using incoherent and short wavelength light. This paper reveals the relationship of diffraction effect and limitation with geometrical configurations and size of eyes. A small eye, such as that of the snake, has advantages for *in vivo* studies of photoreceptor optics and morphology. Photoreceptors in the snake eye are readily imaged because the small eye has higher optical power, higher numerical aperture and relatively higher lateral and axial resolution as compared to the primate eye.

6 Disclaimer

The opinions and assertions contained herein are the private views of the authors, not to be considered as official or reflecting the views of the Department of the Army or the Department of Defense.

In conducting the research described in this report, the investigators adhered to the ''Guide for Care and Use of Laboratory Animals,'' as promulgated by the committee on Revision of the Guide for Laboratory Animal Facilities and Care, Institute of Laboratory Animal Resources, National Academy of Sciences—National Research Council.

Citation of trade names in this report does not constitute an official endorsement or approval of the use of such items.

Acknowledgments

The author appreciates that this research was supported by National Research Council Associate Programs in U.S. Army Medical Research Detachment of Walter Reed Army Institute of Research. The authors gratefully appreciate the technical support of C. Vansice, R. Elliott, A. Akers, and S.S.G. J. Loveday. Also, the authors express deep appreciation to Professor Wolbarsht and Dr. Taboda for reading, and making suggestions and comments on this paper.

References

1. H. Zwick, D. J. Lund, R. Elliott, S. T. Schuschereba, and P. R. Edsall, ''Small eye confocal scanning laser ophthalmoscopy and assessment of retinal damage,'' *Proc. SPIE* **2674**, 80–89 (1996).
2. H. Zwick, D. J. Lund, R. Elliot, and S. T. Schuschereba, ''Confocal spectral ophthalmoscopic imaging of retinal laser damage in small vertebrate eyes,'' *Proc. SPIE* **2393**, 182–188 (1995).
3. H. Zwick, W. R. Elliot, B. E. Stuck, D. J. Lund, S. T. Schuschereba, and G. Li, ''In-vivo laser induced photoreceptor pathology and vas-

cular physiology in small eye animal model,'' *The Proceedings of the International Laser Safety Conference*, Orlando, FL, March, 1997, pp. 182–188.
4. G. Li, H. Zwick, A. Akers, R. Elliott, B. Stuck, J. Lund, and S. Schuscereba, ''High numerical aperture and small eye photoreceptor resolution,'' *OSA Annual Meeting*, Long Beach, CA, October 1997, p. 68.
5. M. F. Land and A. W. Snyder, ''Cone mosaic observed directly through natural pupil of live vertebrate,'' *Vision Res.* **25**, 1519–1523 (1985).
6. D. T. Miller, D. R. Williams, G. M. Morris, and J. Liang, ''Images of cone photoreceptors in the living human eye,'' *Vision Res.* **36**, 1067–1079 (1996).
7. S. Marcos, R. Nararro, and P. Artal, ''Coherent imaging of the cone mosaic in the living human eye,'' *J. Opt. Soc. Am. A* **13**, 897–905 (1996).
8. B. O'Brien, ''Vision and resolution in the central retina,'' *J. Opt. Soc. Am.* **41**, 882–894 (1949).
9. G. Westheimer, ''Modulation thresholds for sinusoidal light distributions on the retina,'' *J. Physiol. (London)* **152**, 67–74 (1960).
10. G. Westheimer and F. W. Campell, ''Light distribution in the image formed by the living human eye,'' *J. Opt. Soc. Am.* **52**, 1040–1045 (1962).
11. J. Krauskopf, ''Light distribution in human retinal images,'' *J. Opt. Soc. Am.* **52**, 1046–1050 (1962).
12. F. W. Campbell and D. G. Green, ''Optical and retinal factors affecting visual resolution,'' *J. Physiol. (London)* **181**, 576–593 (1965).
13. H. B. Barlow, ''Visual resolution and diffraction limit,'' *Science* **149**, 553–555 (1965).
14. F. W. Campbell and R. W. Gubisch, ''Optical image quality of the human eye,'' *J. Physiol. (London)* **186**, 558–578 (1966).
15. R. W. Gubisch, ''Optical performance of the human eye,'' *J. Opt. Soc. Am.* **57**, 407–415 (1967).
16. A. W. Snyder, T. R. Bossomaier, and A. Hughes, ''Optical quality and the cone mosaic,'' *Science* **231**, 499–501 (1986).
17. A. Van Meeteren, ''Calculation on the optical modulation transfer function of the human eye for white light,'' *Opt. Acta* **21**, 395–412 (1974).
18. R. Navarro, P. Artal, and D. R. Williams, ''Modulation transfer of the human eye as a function of retinal eccentricity,'' *J. Opt. Soc. Am. A* **10**, 201–212 (1993).
19. P. Artal, J. Santamaria, and J. Bescos, ''Phase-transfer function of the human eye and its influence on point-spread function and wave aberration,'' *J. Opt. Soc. Am. A* **5**, 1791–1795 (1988).
20. P. Artal and R. Nabarro, ''Monochromatic modulation transfer function of the human eye for different pupil diameters: An analytic expression,'' *J. Opt. Soc. Am. A* **11**, 246–249 (1994).
21. W. J. Smith, *Modern Optical Engineering*, 2nd ed., pp. 327–356, McGraw–Hill, New York (1990).
22. M. Born and E. Wolf, *Principles of Optics*, 6th ed., Chap. 9, Pergamon, Oxford (1980).
23. T. Young, ''On the mechanism of the eye,'' *Philos. Trans. R. Soc. London* **91**, 23–88 (1801).
24. J. K. F. Gauss, *Dioptrische Untersuchungen*, Gottingen (1841).
25. A. Hughes, ''The topography of vision in mammals,'' *Handbook of Sensory Physiology 7(5)*, H. Autrum, R. Jung, W. R. Loewenstein, D. M. MacKay, and H. L. Teuber, Eds., pp. 652–660, Springer, Berlin (1977).
26. A. Safir, *Refraction and Clinical Optics*, pp. 81–132, Harper & Row, Cambridge (1980).
27. D. Troilo, H. C. Howland, and S. J. Judge, ''Visual optics and retinal cone topography in the common marmoset (*Callithrix jacchus*),'' *Vision Res.* **33**, 1301–1310 (1993).
28. A. Hughes, ''A schematic eye for the rat,'' *Vision Res.* **19**, 569–588 (1979).
29. J. G. Sivak, ''The role of the spectacle in the visual optics of the snake eye,'' *Vision Res.* **17**, 293–298 (1977).
30. A. Hughes, ''A schematic eye for the rabbit,'' *Vision Res.* **12**, 123–138 (1972).
31. J. S. Du Pont and J. De Groot, ''A schematic dioptric apparatus for the frog eye (*Rana Esculenta*),'' *Vision Res.* **16**, 803–810 (1976).
32. T. T. Norton and N. A. McBrien, ''Normal development of refractive state and ocular component dimension in the tree shrew (*Tupaia belangeri*),'' *Vision Res.* **32**, 833–842 (1992).
33. N. A. McBrien and T. T. Norton, ''The development of experimental myopia and ocular component dimension in monocularly lid-suture tree shrews (*Tupaia belangeri*),'' *Vision Res.* **32**, 843–852 (1992).
34. J. E. Greivenkamp, J. Schwiegerling, J. M. Miller, and M. D. Mellinger, ''Visual acuity modeling using optical retracing of schematic eyes,'' *Am. J. Ophthalmol.* **120**, 227–240 (1995).
35. D. G. Green, M. K. Powers, and M. S. Banks, ''Depth of focus, eye size and visual acuity,'' *Vision Res.* **20**, 827–835 (1980).
36. C. A. Taylor and B. J. Thompason, ''Attempt to investigate experimentally the intensity distribution near the focus in the error-free diffraction patterns of circular and annular apertures,'' *J. Opt. Soc. Am. A* **48**, 844–850 (1958).
37. D. E. Stoltzman, ''The perfect point spread function,'' *Applied Optics and Optical Engineering*, R. Shannon and J. Wyant, Eds., Vol. IX, pp. 111–148, Academic, New York (1983).